



Investigation of Structures, Vibrational Spectra, and Morphological Characteristics of Undoped and Cobalt-doped Ni-Zn Ferrite

J Utomo^{1*}, R Kurniawan¹, M R A Taqwa¹, B R Kurniawan¹, N E A Wahyuni¹, and A Sukkaew²

Received
24 April 2022

Revised
05 June 2022

Accepted for Publication
05 July 2022

Published
11 July 2022

¹ Department of Physics, Faculty of Mathematics and Natural Sciences, Universitas Negeri Malang, Jl. Semarang 5, Malang, 65145, Indonesia.

² Department of Renewable Energy Technology, Faculty of Science Technology and Agriculture, Yala Rajabhat University, Satang Sub-district, Muang District, 95000, Thailand.

*E-mail: joko.utomo.fmipa@um.ac.id



This work is licensed under a [Creative Commons Attribution-ShareAlike 4.0 International License](https://creativecommons.org/licenses/by-sa/4.0/)

Abstract

Undoped and Co-doped Nickel Zinc ferrite ($\text{NiZnFe}_2\text{O}_4$) have been successfully prepared using the coprecipitation method with the further annealing treatment at 600 °C. The structure, image, and vibrational spectra of the materials were investigated respectively by XRD, TEM, and FTIR characterizations. Based on XRD characterization results, both undoped and Co-doped Ni – Zn ferrite possesses a single-phase formation, namely spinel structure without any impurities from other phases. The lattice parameters of Co-doped Ni – Zn ferrite is 8.419 nm which is higher than undoped Ni – Zn ferrite (8.409 nm). Meanwhile, the average particle size obtained based on the results of the TEM characterization is 14.4 nm with slight agglomeration. The results of FTIR characterization on all samples provide information on the presence of metal ion vibrations at frequency bands about 493.78 cm^{-1} located at the tetrahedral and 514.99 cm^{-1} occupied at octahedral sites. Those frequency ranges confirmed that both samples have spinel structures.

Keywords: Ni – Zn ferrite, Co-doped, ferrite, coprecipitation.

1. Introduction

Magnetic nanoparticles have attracted much attention from researchers because of their wide applications, including in data storage, biomedicine, absorbent of electromagnetic radiation, and catalysts [1]–[3]. That is according to their unique properties, such as good chemical stability, low magnetic coercivity, high electrical permeability, and resistivity [4]. As a result, the use of magnetic nanoparticles, particularly spinel ferrite, has tremendously increased in the present age. Spinel ferrite has the chemical formula MeFe_2O_4 , where Me is a bivalent metal (Me = Ni, Co, Mg, Fe, Zn, and Mn) which has a cubic structure with a space grub of Fd-3m [5], [6].

One of the ferrite nanoparticles currently being studied due to its potential properties is Nickel Zinc (Ni – Zn) ferrite which is suitable for specific applications like transformers and inductors [7]. Nevertheless, Ni – Zn ferrite has not been applied massively for those modern electronic devices because they require higher performance of the materials. It can be achieved through developing modularization, high-frequency, and miniaturization. The enhancement of the characteristic of Ni – Zn ferrite is mainly affected by some considerations such as the chosen synthesis method and the dopant of bivalent metal [8], [9].

Based on the previous research, Shahane *et al.* [2] investigated Ni – Zn ferrite nanoparticles, and the results informed that the single crystalline was formed through chemical coprecipitation. In addition, they showed that the lower Ni content in the prepared sample was, the less value of saturation magnetization was obtained. Consequently, the anisotropy constant of those materials is lower, as well as the saturation magnetization. The Co addition of Ni – Zn ferrite nanoparticles could enhance the anisotropy value of the crystal that is related to the device's performance [10]. Moreover, the magnetic characteristics, anisotropy constant included, of Ni – Zn ferrites are mainly affected by the crystal

structures, particularly particle size and their morphologies [11]–[13]. Various synthesis methods have been conducted to produce Ni – Zn ferrites, such as hydrothermal, sol-gel, coprecipitation, and others [14]–[16].

According to the above relevant studies, we provide comprehensive information of Ni – Zn ferrites and Co-doped Ni – Zn ferrites on the structural characteristics and morphology. Also, the relation between their characteristics can be used as a reference for future applications particularly in modern electronic devices using potential material either Ni – Zn ferrites or Co-doped Ni – Zn ferrites.

2. Method

Undoped and Co-doped Ni – Zn ferrite had been prepared using the coprecipitation method. Initial precursors used nickel chloride, zinc sulfate, cobalt chloride, iron chloride, and sodium hydroxide (NaOH). Firstly, the molarity comparison of bivalent metal (Ni-Zn-Co) and trivalent metal (Fe) was determined as 1:2, respectively, to measure the mass of each precursor. The 0.4 M solution of iron chloride and 0.2 M solution of nickel chloride, zinc sulfate, or added cobalt chloride were prepared in two separate 25 ml of distilled water and then mixed for 5 minutes. Then, the mixed solution was added to 3.37 ml HCL as a catalyst to enhance the chemical reaction and dissolved until homogenous.

In the next step, the dissolved solution was added wisely to the 3 M of NaOH to obtain the liquid precipitate. During the process, the liquid precipitate was stirred with the synthesis temperature of 90 °C for 60 minutes and centrifuged at 1000 rpm. The pH of the obtained solution was constantly monitored at approximately 12. Then, in addition, the liquid precipitate was cleaned with distilled water 4 – 6 times to minimize the presence of unreacted dissolved salts during the coprecipitation process. Afterwards, the product was dried for 4 hours in a furnace at 90 °C synthesis temperature to obtain powder after grinding. Then, the dried powder was annealed at 600 °C for 4 hours to obtain the desired samples. Finally, the dried sample after the annealing process was obtained and characterized by X-ray Diffractometer (XRD), Fourier Transform Infra-Red (FTIR) spectroscopy, and Transmission Electron Microscope (TEM) to investigate the structural, vibrational, and morphological properties of the samples, respectively.

3. Result and Discussion

3.1. Structural Characteristics

Figure 1 reveals the diffraction pattern of prepared undoped and Co-doped Ni – Zn ferrite ($\text{NiZnFe}_2\text{O}_4$). Based on Figure 1a, all samples have high crystallinity with cubic spinel structure without the addition of impurities from the other phases. In addition, all obtained samples show well-crystallized according to the high diffraction peak intensity, particularly at the reflection plane (331) (Figure 1b). That is because all samples have no amorphous detected by XRD results. All samples represented by the characteristic of appeared diffraction peaks which are (220), (331), (400), (422), (511), (440), and (310)

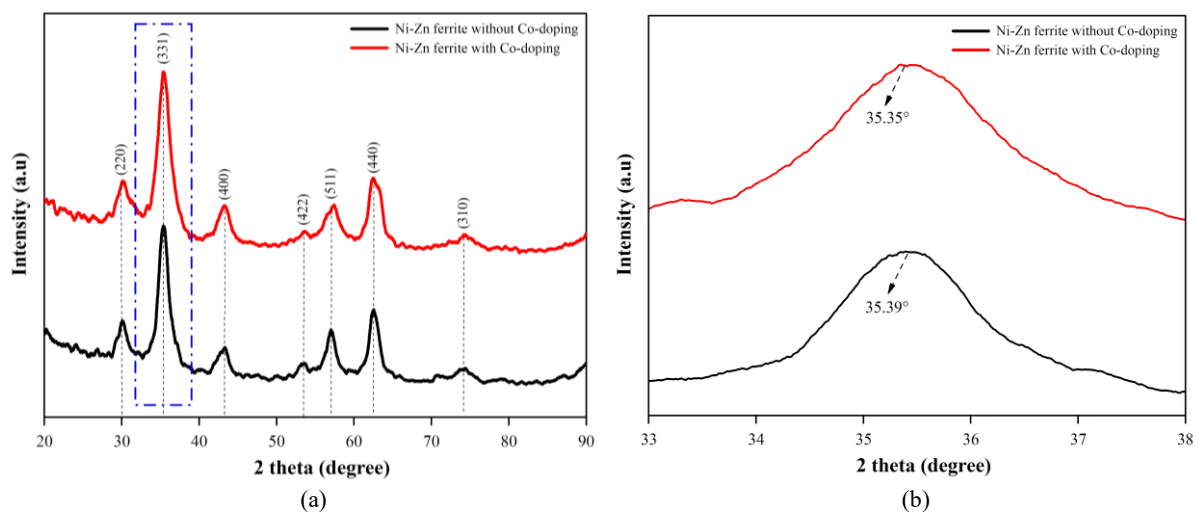


Figure 1. (a) The XRD pattern of undoped and Co-doped Ni – Zn ferrite, (b) Peak shifting (331) of XRD pattern.

Table 1. Microstructure of undoped and Co-doped Ni – Zn ferrite.

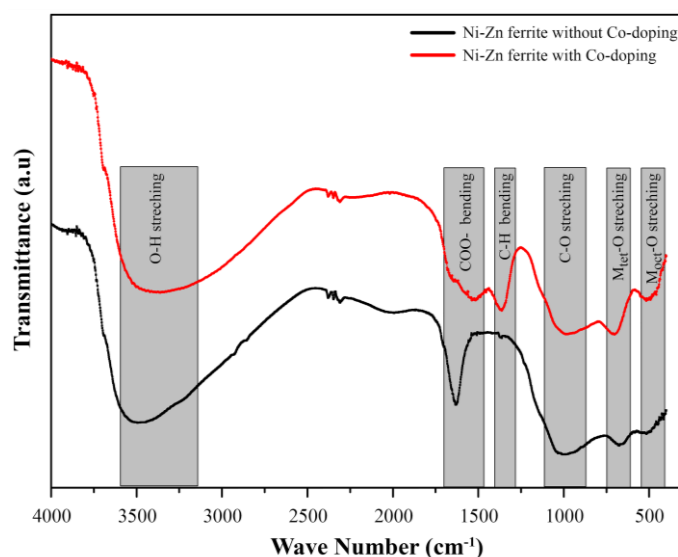
NiZnFe ₂ O ₄	Constant Parameter (Å)	Crystallite Size (nm)	X-ray Density (10 ³ kg/cm ³)	Strain
Co-undoped	8.409	6.85	5.31	0.0665
Co-doped	8.419	6.37	5.29	0.0717

confirmed to the JCPDS standard no 74-2081 [6]. Both samples', the most dominant diffraction peak is located at a diffraction angle of nearly 35.35° with the reflection plane of (331). This prominent angle diffraction is the main characteristic of spinel structure. The diffraction peak of Co-doped Ni – Zn ferrite experiences a shift to a smaller diffraction angle, indicating a change in the position of the atoms in a lattice. The shift of the diffraction peak affects the change in the value of the constant parameter, strain, and crystallite size. Furthermore, the shift of a smaller diffraction peak (331) might be attributed to the expansion of the lattice volume. In more detail, the structural parameters of "with and without Co content" in Ni – Zn ferrite are revealed in Table 1.

Based on Table 1, the lattice parameter of Co-doped Ni – Zn ferrite is slightly higher than undoped Ni – Zn ferrite. This phenomenon can be related to the ionic radii of Ni²⁺ (0.69 Å) being smaller than the ionic radii of Co²⁺ (0.745 Å) in Co-doped Ni – Zn ferrite [13], [17]. Meanwhile, the value of crystallite size and x-ray density of Co-doped Ni – Zn ferrite are smaller than undoped. One of the factors that cause a tendency to change in crystallite size is related to the chemical composition of Co, Ni, and Zn involved in the ferritization process. Another factor affecting the smaller crystallite size of Co-doped Ni – Zn ferrite is the high strain value of the crystal. In addition, the strain of Co-doped Ni – Zn ferrite is higher than undoped. The strain parameter can be represented as a sign of imperfection in a crystal. The higher the strain value (Co-doped Ni – Zn ferrite), the greater the crystal's imperfections appeared.

3.2. FTIR Spectra

The vibrational characteristic of undoped and cobalt-doped nickel-zinc ferrite (NiZnFe₂O₄) at room temperature is provided in Figure 2. The fundamental frequency bands at approximately 511.62 cm⁻¹ and 660.86 cm⁻¹ correspond to metal-oxide at octahedral and tetrahedral sites, respectively. This infrared absorption range represents cubic spinel structure and these samples are well crystallized. The absorption band of around 1372.06 cm⁻¹ and 1623.12 cm⁻¹ attributes to the vibrational modes of C – H and COO – bonds, respectively [1], [4]. Moreover, the FTIR frequency bands at about 3492.44 cm⁻¹ for both samples correspond to symmetric vibration of O – H stretching [18].

**Figure 2.** FTIR spectra of undoped and Co-doped Ni – Zn ferrite.

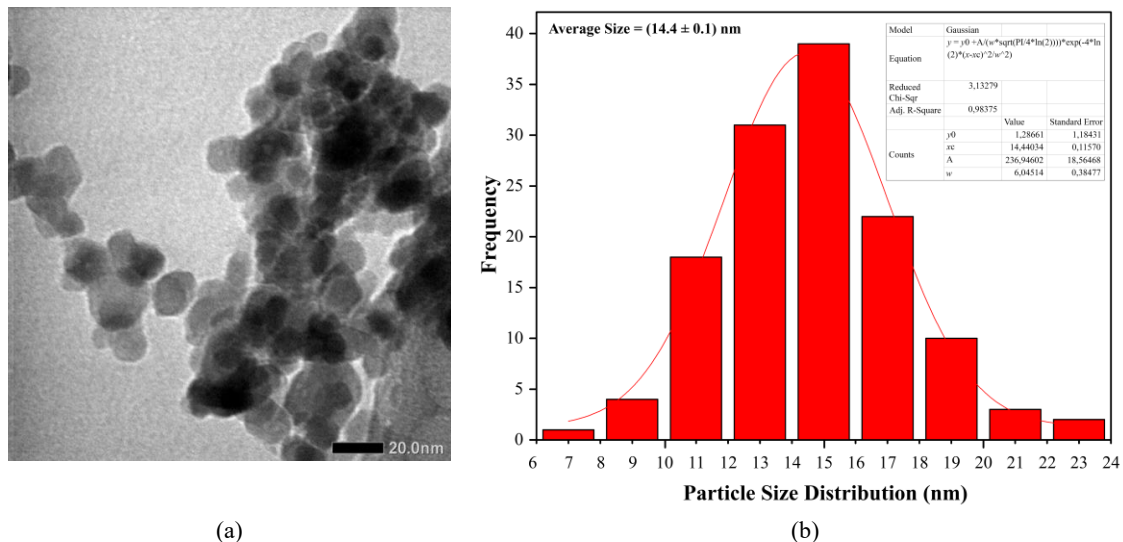


Figure 3. (a) The morphology and (b) Histogram of particles-size distribution of Co-doped Ni – Zn ferrite.

3.3. Morphological Studies

Figure 3 displays the TEM micrograph of Co-doped Ni – Zn ferrite annealed at 600 °C. The shape of particle distribution is nearly spherical. In addition, the particle distribution tends to agglomerate due to the high annealing temperature applied to the sample. Agglomeration of particles might also be attributed to Van-der Waals and electrostatic forces creating bigger particles from mutual interaction between tiny particles [19], [20]. Based on the TEM analysis, the average particle distribution is 14.4 nm. Moreover, a small homogeneous image of particles is obtained from this sample. The particle size and shape of particles are in good agreement with the previous research conducted [21].

4. Conclusion

Undoped and Co-doped Ni – Zn ferrite were prepared by coprecipitation technique with a further temperature of 600 °C. All samples have been crystallized with the cubic spinel structures based on the XRD result. The lattice parameter of Co-doped is higher than undoped in Ni – Zn ferrite. The shape of the prepared sample is nearly spherical, with the average diameter of particles being about 14.4 nm. In addition, the vibrational spectra at 511.62 cm^{-1} and 660.86 cm^{-1} correspond to metal-oxide at octahedral and tetrahedral sites, respectively. This infrared absorption range represents a cubic spinel structure. To sum up, the fundamental parameters of potential materials, namely undoped and Co-doped Ni – Zn ferrite, have been studied explicitly. Further research will focus on finding optimum parameters such as electrical, magnetic, and needed properties related to electronic device applications.

Acknowledgment

This work is fully funded by the competitive Grant Project of PNPB Universitas Negeri Malang (No 4.3.13/UN32/KP/2021).

References

- [1] A. Manohar, C. Krishnamoorthi, C. Pavithra, and N. Thota, “Magnetic hyperthermia and photocatalytic properties of MnFe_2O_4 nanoparticles synthesized by solvothermal reflux method,” *J. Supercond. Nov. Magn.*, vol. 34, no. 1, pp. 251–259, 2021, doi: [10.1007/s10948-020-05685-x](https://doi.org/10.1007/s10948-020-05685-x).
- [2] G. S. Shahane, A. Kumar, M. Arora, R. P. Pant, and K. Lal, “Synthesis and characterization of Ni-Zn ferrite nanoparticles,” *J. Magn. Magn. Mater.*, vol. 322, no. 8, pp. 1015–1019, 2010, doi: [10.1016/j.jmmm.2009.12.006](https://doi.org/10.1016/j.jmmm.2009.12.006).
- [3] S. Zhao, C. Wang, and B. Zhong, “Optimization of electromagnetic wave absorbing properties for Ni-Co-P/GNs by controlling the content ratio of Ni to Co,” *J. Magn. Magn. Mater.*, vol. 495, p. 165753, 2020, doi: [10.1016/j.jmmm.2019.165753](https://doi.org/10.1016/j.jmmm.2019.165753).

- [4] P. L. Leng, M. G. Naseri, E. Saion, A. H. Shaari, and M. A. Kamaruddin, "Synthesis and characterization of Ni-Zn ferrite nanoparticles ($\text{Ni}_{0.25}\text{Zn}_{0.75}\text{Fe}_2\text{O}_4$) by thermal treatment method," *Adv. Nanoparticles*, vol. 02, no. 04, pp. 378–383, 2013, doi: [10.4236/anp.2013.24052](https://doi.org/10.4236/anp.2013.24052).
- [5] A. Yadav and D. Varshney, "Structural and dielectric properties of copper-substituted Mg-Zn spinel ferrites," *J. Supercond. Nov. Magn.*, vol. 30, no. 5, pp. 1297–1302, 2017, doi: [10.1007/s10948-016-3931-2](https://doi.org/10.1007/s10948-016-3931-2).
- [6] S. B. Gopale, G. N. Kakade, G. D. Kulkarni, V. Vinayak, S. P. Jadhav, and K. M. Jadhav, "X-ray diffraction, infrared and magnetic studies of NiFe_2O_4 nanoparticles," *J. Phys. Conf. Ser.*, vol. 1644, no. 1, p. 012010, 2020, doi: [10.1088/1742-6596/1644/1/012010](https://doi.org/10.1088/1742-6596/1644/1/012010).
- [7] A. Kumar *et al.*, "Structural and magnetic studies of the nickel doped CoFe_2O_4 ferrite nanoparticles synthesized by the chemical co-precipitation method," *J. Magn. Magn. Mater.*, vol. 394, pp. 379–384, 2015, doi: [10.1016/J.JMMM.2015.06.087](https://doi.org/10.1016/J.JMMM.2015.06.087).
- [8] M. A. Ali *et al.*, "Magnetic properties of Sn-substituted Ni-Zn ferrites synthesized from nano-sized powders of NiO, ZnO, Fe_2O_3 , and SnO_2 ," *Chinese Phys. B*, vol. 26, no. 7, p. 077501, 2017, doi: [10.1088/1674-1056/26/7/077501](https://doi.org/10.1088/1674-1056/26/7/077501).
- [9] J. Bobic, M. Vijatovic-Petrovic, and B. Stojanovic, "Aurivillius $\text{BaBi}_4\text{Ti}_4\text{O}_{15}$ based compounds: Structure, synthesis and properties," *Process. Appl. Ceram.*, vol. 7, no. 3, pp. 97–110, 2013, doi: [10.2298/pac1303097b](https://doi.org/10.2298/pac1303097b).
- [10] Z. C. Zhong *et al.*, "Influence of Nd substitution on the structural, magnetic and electrical properties of NiZnCo ferrites," *Ceram. Int.*, vol. 47, no. 7, pp. 8781–8786, 2021, doi: [10.1016/j.ceramint.2020.11.243](https://doi.org/10.1016/j.ceramint.2020.11.243).
- [11] J. A. Hwang, M. Choi, H. S. Shin, B. K. Ju, and M. P. Chun, "Structural and magnetic properties of NiZn ferrite nanoparticles synthesized by a thermal decomposition method," *Appl. Sci.*, vol. 10, no. 18, p. 6279, 2020, doi: [10.3390/APP10186279](https://doi.org/10.3390/APP10186279).
- [12] L. Z. Li, X. X. Zhong, R. Wang, X. Q. Tu, and L. He, "Effects of Al substitution on the properties of NiZnCo ferrite nanopowders," *J. Mater. Sci. Mater. Electron.*, vol. 29, no. 9, pp. 7233–7238, 2018, doi: [10.1007/s10854-018-8712-1](https://doi.org/10.1007/s10854-018-8712-1).
- [13] A. Maqsood, K. Khan, M. Anis-Ur-Rehman, and M. A. Malik, "Spectroscopic and magnetic investigation of NiCo nanoferrites," *J. Alloys Compd.*, vol. 509, no. 27, pp. 7493–7497, 2011, doi: [10.1016/j.jallcom.2011.04.092](https://doi.org/10.1016/j.jallcom.2011.04.092).
- [14] E. Leal *et al.*, "Structural, textural, morphological, magnetic and electromagnetic study of Cu-doped NiZn ferrite synthesized by pilot-scale combustion for RAM application," *Arab. J. Chem.*, vol. 13, no. 11, pp. 8100–8118, 2020, doi: [10.1016/j.arabjc.2020.09.041](https://doi.org/10.1016/j.arabjc.2020.09.041).
- [15] C. Virlan, F. Tudorache, and A. Pui, "Tertiary NiCuZn ferrites for improved humidity sensors: A systematic study," *Arab. J. Chem.*, vol. 13, no. 1, pp. 2066–2075, 2020, doi: [10.1016/j.arabjc.2018.03.005](https://doi.org/10.1016/j.arabjc.2018.03.005).
- [16] P. Chavan *et al.*, "Studies on electrical and magnetic properties of Mg-substituted nickel ferrites," *J. Electron. Mater.*, vol. 46, no. 1, pp. 188–198, 2017, doi: [10.1007/s11664-016-4886-6](https://doi.org/10.1007/s11664-016-4886-6).
- [17] J. Utomo, A. K. Agustina, E. Suharyadi, T. Kato, and S. Iwata, "Effect of Co concentration on crystal structures and magnetic properties of $\text{Ni}_{1-x}\text{Co}_x\text{Fe}_2\text{O}_4$ nanoparticles synthesized by co-precipitation method," *Integr. Ferroelectr.*, vol. 187, no. 1, pp. 194–202, 2018, doi: [10.1080/10584587.2018.1445348](https://doi.org/10.1080/10584587.2018.1445348).
- [18] L. Z. Li, X. Q. Tu, R. Wang, and L. Peng, "Structural and magnetic properties of Cr-substituted NiZnCo ferrite nanopowders," *J. Magn. Magn. Mater.*, vol. 381, pp. 328–331, 2015, doi: [10.1016/j.jmmm.2015.01.020](https://doi.org/10.1016/j.jmmm.2015.01.020).
- [19] Y. K. Dasan, B. H. Guan, M. H. Zahari, and L. K. Chuan, "Influence of La^{3+} substitution on structure, morphology and magnetic properties of nanocrystalline Ni-Zn ferrite," *PLoS One*, vol. 12, no. 1, pp. 1–14, 2017, doi: [10.1371/journal.pone.0170075](https://doi.org/10.1371/journal.pone.0170075).
- [20] S. C. Endres, L. C. Ciacchi, and L. Mädler, "A review of contact force models between nanoparticles in agglomerates, aggregates, and films," *J. Aerosol Sci.*, vol. 153, p. 105719, 2021, doi: [10.1016/J.JAEROSCI.2020.105719](https://doi.org/10.1016/J.JAEROSCI.2020.105719).
- [21] J. Utomo, A. K. Agustina, and E. Suharyadi, "Annealing temperature effect on structural, vibrational and optical properties of $\text{Co}_{0.8}\text{Ni}_{0.2}\text{Fe}_2\text{O}_4$ nanoparticles," *IOP Conf. Ser. Mater. Sci. Eng.*, vol. 432, no. 1, p. 012033, 2018, doi: [10.1088/1757-899X/432/1/012033](https://doi.org/10.1088/1757-899X/432/1/012033).